Acta Polytechnica **62**(6):627–638, 2022
https://doi.org/10.14311/AP.2022.62.0627

Published by the Czech Technical University in Prague

THEORETICAL ANALYSIS OF THE INFLUENCE OF THE CHEVRON INCLINATION ANGLE ON THE THERMAL PERFORMANCE OF A GASKET PLATE HEAT EXCHANGER

Élcio Nogueira

State University of Rio de Janeiro, Department of Mechanic and Energy, Rio de Janeiro, Brazil
correspondence: elcionogueira@hotmail.com

Abstract.

Different models are applied for an experimental and theoretical determination of the thermal and hydraulic performance of gasket plate heat exchanger. One of the relevant aspects of recent works is the influence of the chevron inclination angle between the heat exchanger plates. This work aims to analyse the impact of the chevron inclination angle by applying an effective concept in a sunflower vegetable oil cooler. Comparisons are made with theoretical and experimental results from the literature for works that consider angles of inclination equal to 30°, 45°, and 60°. An analysis model that does not consider the inclination angle as an explicit parameter is included for comparison purposes. In addition to the angle of inclination, two other parameters, the mass flow rate of the cold fluid (water) and the number of plates, are considered crucial for determining and analysing the results. Nusselt number, global heat transfer coefficient, effectiveness, heat transfer rate, and outlet temperatures for hot and cold fluids are presented in a graphical format. The results point to the need to improve models applied to gasket plate heat exchangers concerning the influence of the inclination angle since there are significant differences between those obtained and analysed in this work

Keywords: Gasket plate heat exchanger, chevron inclination angle, vegetable oil cooler, theoretical analysis, second law of thermodynamics.

1. Introduction

Researchers have made numerous efforts to increase the performance of gasket plate heat exchangers; however, regarding the influence of the inclination angle of the chevron plates, there are different procedures recommended for determining the performance of the gasket plate heat exchanger. The work analyses three of these procedures [1–3], which have different degrees of refinement. The objective is to present the observed differences and emphasize them so that the differences between them are evident. To achieve the goal, two aspects that strongly influence the performance of the heat exchanger are included in the present analytical model: the number of plates and the mass flow rate of the working fluid. The inclusion of these two aspects, added to the inclination angle, emphasizes the significant differences between the procedures under analysis.

The present work theoretically analyses the influence of the three abovementioned parameters, but with a greater emphasis on the aspect related to the inclination angle. This parameter has been the object of a recent analysis [1, 2] through different methodologies, that is, a model that applies computational fluid dynamics (CFD) and another, more comprehensive, that uses a semi-analytical model coupled to an experimental procedure in an industrial plant. These procedures contrast with many works in which the influence of the angle of inclination is not considered in determining the thermal performance of a gasket plate heat exchanger. Instead, most works use the Kumar correlation to determine the Nusselt number, as mentioned by Kacaç et al. [3].

In summary, the present work aims to analyse the impact of the chevron inclination angle on a Gasketed Plate Heat Exchanger, applying the concept of effectiveness in a sunflower vegetable oil cooler. The points under analysis are equal to 30°, 45°, and 60°.

The gasket plate heat exchanger consists of a package of thin corrugated metal plates pressed together, with the plates of the heat exchanger arranged so that the two fluids flow alternately in the channels. The heat exchanger's geometry enables high heat transfer coefficients and has low fabrication and maintenance costs. In addition, gasket plate heat exchangers have a solid and robust structure and are very effective for heat transfer. The search to improve the performance of these types of exchangers continues today, and experiments are carried out with the introduction of chevron-type plates. The improvement in the thermal performance depends on reliable correlations for Nusselt number determination and, consequently, accurate determination of heat transfer coefficients in the heat exchanger. This determination is vital for the design of industrial plants and the analysis of actual installations.

The work carried out by Skočilas and Palaziuk [1] applies computational fluid dynamics (CFD) to determine heat transfer through a chevron plate. They

provide expressions for tilt angle-dependent Nusselt number and use experimental results from the literature and results obtained by a numerical simulation to compare with the developed model. They state that the model of turbulent water flow between two corrugated chevron plates can provide relevant information about the momentum transfer and thermal diffusivity process. They fit the developed model using a numerical model and experimental data. They consider that the model can predict essential performance characteristics in plate heat exchangers concerning the dimensions, angles of inclination of the corrugations, etc. In addition, they claim that the performed simulation demonstrates the advantages of using chevron ripples as compared to using smooth plates since they allow high heat transfer coefficients. They conclude by saying that the simulation results can help find geometries with the lowest possible value of hydraulic resistance.

Neagu and Konsag [2] validate Lévêque's semi-analytical model using experimental data obtained in four heat exchangers of different sizes. The model considers the flow in the cell's sine duct in the furrow direction, and Nusselt numbers are calculated considering the construction of the channels. The model was validated for corrugation inclination angle relative to vertical direction equal to 30º. The analysis of relative errors and the statistical analysis concluded for predicting Nusselt number in gasket plate exchangers, showed promising results.

The correlation for the Nusselt number independent of the chevron plate inclination angle obtained by Kumar, referenced by Kakaç et al. [3], was also used in the analysis.

Élcio Nogueira [4] uses the concept of entropy generation to analyse the thermo-hydraulic performance of a gasket plate heat exchanger for cooling vegetable oil and uses volumetric fractions of non-spherical nanoparticles in a water-ethylene glycol mixture as a coolant. He concludes that it is possible to work with relatively low flow rates using non-spherical nanoparticles, emphasizing platelet-shaped nanoparticles. The analysis of thermal entropy generation versus viscous entropy generation shows that high flow rates dissipate a large part of the valuable energy available and do not contribute to oil cooling, increasing the operating cost of the heat exchanger.

Tovazhnyanskyy et al. [5] present the development and study of constructing a specially welded plate heat exchanger. They investigate heat transfer and hydraulic performance in a single-pass model under laboratory conditions, and propose an equation that relates the effectiveness and the number of thermal units. They develop a mathematical model for multi-pass heat exchangers from the results obtained, and validate the model through results obtained in an industrial prototype confirming the reliability and efficiency of the heat exchanger under analysis compared to a tubular heat exchanger. In addition, they developed a method that makes it possible to determine the height of the undulations and the number of passes for specified operating conditions.

Nguyen et al. [6] present a study where nickel, copper, and silver electrolytic coating is applied to stainless steel plate heat exchangers to improve the thermo-hydraulic performance. An experiment was conducted where the efficiency was evaluated using the global heat transfer coefficient, friction factor, number of transfer units, and effectiveness. It was found that all coated plate heat exchangers showed an increase in performance, especially for silver, followed by copper and nickel. Finally, they pointed out that the study shows a potential regarding applications in environments of severe and corrosive wear or with hygiene requirements.

Kumar and Singh [7] conducted an experimental study on a plate heat exchanger and presented thermal and hydraulic performance results with Reynolds numbers ranging between 800 and 5900. They use a chevron plate with an angle equal to 60° in isothermal or non-isothermal conditions. They compare the Nusselt number developed based on experimental data with analytical and numerical expressions from the literature, and conclude that the global heat transfer coefficient increases with the Reynolds number and decreases with the number of plates. They state that considering uniform flux distribution for many plates is undesirable.

Grigore et al. [8] present a theoretical and experimental study and perform a numerical simulation for a counterflow plate heat exchanger using the finite element method. They develop an iterative model that considers characteristics related to the channel geometry and determines heat transfer and fluid flow results. They conclude that the developed model agrees with experimental results, despite being a complex and labour-intensive simulation and presenting an excessive consumption of computational resources. In addition, they claim that the numerical simulation does not capture the influence of the angle and height of the ripple. However, the model offers a good understanding of the temperature distribution and fluid flow in turbulent conditions.

Jamil et al. [9] developed a theory to analyse heat exchangers through exergoeconomic concepts and normalised sensitivity analysis. The model allows the investigation of thermodynamic effects associated with fiscal parameters and is more comprehensive and significant than the conventional thermodynamic or economic analyses used separately. They present a practical example in a plate exchanger used in a desalination system. The sensitivity analysis demonstrates that the most critical input variables for determining the heat transfer rate are the mass water flows and the salinity. Essential variables of input for the cost of operation are the mass flow rates of hot and cold fluids, followed by the cost of electricity, interest rate, and pump efficiency. The parametric analysis demon-

strates that the $h/\Delta P$ ratio decreases with increasing Reynolds number and that the cold stream outlet cost is higher for $\beta = 30°$ than for $\beta = 60°$.

D. dos S. Ferreira et al. [10] study the application of the Wilson-Plot method for analysis and verify if the fluid inlet temperatures significantly influence the thermal behaviour of a plate heat exchanger. The research is performed by varying the inlet temperature and the mass flow of the hot fluid with the mass flow of the cold fluid, fixed. The experimental data presented a relative error of less than 15 %, within the scope of uncertainties of the analysed correlations. It is concluded that the Wilson plotting method is highly effective for analysing the thermal behaviour of a plate heat exchanger.

Mota et al. [11] present two methods for analysing the thermal and hydraulic performance. The first simulates a configuration of a heat exchanger operating in a steady state. The parameters considered in the analysis are the number of channels, number of passes, the locations of the connections, and the type of flow. The second model applies to multi-pass heat exchangers with a large number of plates, which can be reduced to a single pass. In this particular case, they established that most multi-pass plate heat exchangers are equivalent to combinations of single-pass exchangers. They observed that the first model is limited to heat exchangers with a large number of plates and that industrial heat exchangers have more than 40 thermal plates. They highlight the advantage of using the first model as it has an applicability to any configuration. However, the implementation is highly complex, contrary to the second approach.

Anusha and Kishore [12] present an experimental work in a heat exchanger with 249 stainless steel welded metal sheets used in hydraulic cooling. They determine the correlation for Nusselt number as a function of Reynolds number, Prandtl number, and chevron angle. They get results for the heat transfer coefficient, overall heat transfer coefficient, and effectiveness. Graphical results are used to demonstrate the performance of the Gasket Plate Heat Exchanger. They conclude that the maximum effectiveness for counterflow arrangement is equal to 0.949 and that with increasing Reynolds number from 20 to 60, the Nusselt number increased by 10.01 %, the friction factor decreased by 25.7 %, the overall heat transfer coefficient increased by 10.44 %, and the effectiveness increased by 12.53 %.

Khond et al. [13] worked to optimise the performance of the plate heat exchanger by reducing the number of plates and, for that, they present a mathematical model that allows to reach the optimum in certain operational restrictions. The results obtained through applying the mathematical model demonstrate that the effect of the initial and final plates and the transverse flow distribution are considerable and affect the performance of the heat exchanger. They conclude that the model proposed in the work meets the thermal and hydraulic demand and makes it possible to determine the smallest number of plates necessary for the adequate performance of the heat exchanger. However, they note that a more advanced algorithm is needed to achieve greater precision in determining the minimum number of plates.

In this context, the present work aims to analyse the impact of the chevron inclination angle in a Gasket Plate Heat Exchanger by applying the effective concept in a sunflower vegetable oil cooler. The tips under analysis are equal to 30°, 45°, and 60°.

2. Methodology

The geometric characteristic and physical parameters of the heat exchangers used in the present work were those tested by Neagu and Koncsag [2]. The relevant fact regarding the models is that Skočilas and Palaziuk [1] used water as the working fluid and two chevron plates for the numerical simulation (CFD). The work developed by Neagu and Koncsag [2] was theoretical and experimental in an industrial plant, using water and vegetable oil as working fluids, and presented comparisons with relative errors below 20 %.

The fluids that exchange heat are water and sunflower vegetable oil. The water at 30° is used to cool vegetable oil that enters the heat exchanger at a temperature of 110°. The heat exchanger used for the analysis uses 63 plates, and the original chevron plate has an angle of inclination equal to 30°. The empirical expressions used to determine the Nusselt number were taken from three independent works [1–3]. Sunflower properties were taken from numerical tables provided in the literature [13] and determined through 3^{rd} and 4^{th}-degree polynomial interpolations (Equations (1)–(5)). Angles of 45° and 60° were introduced in the analysis for comparison purposes. The results independent of the inclination angle are arbitrarily referenced as the angle of inclination equal to 0°. Two parameters independent of the angle of inclination, the flow rate of the cold fluid and the number of plates of the heat exchanger, are predominant for determining the thermal performance. Therefore, their variations were included in the analysis.

Figure 1 shows geometric features of a chevron-type plate. Recent works [1, 2] use the chevron angle, β, the corrugation depth, b, and the corrugation wavelength, l, to look for local influences that can improve empirical expressions for the Nusselt number, which generally depends on the Reynolds number and the Prandtl number. In the present work, fixed values are adopted for b and l. In contrast, in most simulations, empirical expressions for Nusselt number are used in which the chevron angle appears explicitly.

Table 1 presents properties for the fluids used in this work as a function of average temperatures. Water is used to cool the vegetable oil in the case under analysis.

$Tc_i = 30\,°\text{C}$ and $Th_i = 110\,°\text{C}$ are the inlet temperatures of water and vegetable oil. $\overline{T}c = 35\,°\text{C}$,

	ρ [kg/m^3]	k [W/(m K)]	Cp [J/(kg K)]	μ [kg/(m s)]	ν [m/s^2]	α [m/s^2]	Pr
Water	993.80	0.610	4186	$0.725 \cdot 10^{-3}$	$7.29 \cdot 10^{-7}$	$1.47 \cdot 10^{-7}$	4.96
Sunflower	913.00	0.163	2346	$11.54 \cdot 10^{-3}$	$1.26 \cdot 10^{-5}$	$0.76 \cdot 10^{-7}$	166

Table 1. Physical properties for cold (water) and hot (sunflower vegetable oil) fluids.

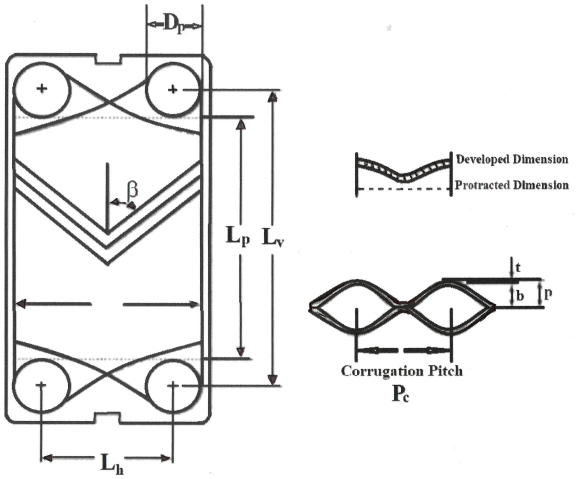

Figure 1. Basic geometrical dimensions of chevron corrugated plate heat exchanger [2].

$\overline{T}h = 75\,^{\circ}\mathrm{C}$ and $\overline{T}_W = 55\,^{\circ}\mathrm{C}$.

$$\begin{aligned}\rho_h &= 920.8893939 - 0.09046037296\,\overline{T}_h \\ &\quad - 0.0003712121212\,{\overline{T}_h}^2 \\ &\quad + 2.331002331 \cdot 10^{-6}\,{\overline{T}_h}^3,\end{aligned} \tag{1}$$

$$\begin{aligned}\mu_h &= 0.144681007 - 0.00571479528\,\overline{T}_h \\ &\quad + 9.81172771 \cdot 10^{-5}\,{\overline{T}_h}^2 \\ &\quad - 7.880585664 \cdot 10^{-7}\,{\overline{T}_h}^3 \\ &\quad + 2.402607809 \cdot 10^{-9}\,{\overline{T}_h}^4,\end{aligned} \tag{2}$$

$$\begin{aligned}\mu_W &= 0.144681007 - 0.00571479528\,\overline{T}_W \\ &\quad + 9.81172771 \cdot 10^{-5}\,{\overline{T}_W}^2 \\ &\quad - 7.880585664 \cdot 10^{-7}\,{\overline{T}_W}^3 \\ &\quad + 2.402607809 \cdot 10^{-9}\,{\overline{T}_W}^4,\end{aligned} \tag{3}$$

$$\begin{aligned}k_h &= 0.1595212121 + 7.626262626 \cdot 10^{-5}\,\overline{T}_h \\ &\quad - 5.303030303 \cdot 10^{-7}\,{\overline{T}_h}^2 \\ &\quad + 2.5252525 \cdot 10^{-9}\,{\overline{T}_h}^3,\end{aligned} \tag{4}$$

$$\begin{aligned}Cp_h &= 2046.651515 + 3.511130536\,\overline{T}_h \\ &\quad - 0.005606060606\,{\overline{T}_h}^2 \\ &\quad + 9.906759907 \cdot 10^{-6}\,{\overline{T}_h}^3,\end{aligned} \tag{5}$$

where ρ_h is the specific mass (density) of the hot fluid, μ_h is the dynamic viscosity of the hot fluid, μ_W is the dynamic viscosity of the hot fluid at the surface, k_h is the thermal conductivity of the hot fluid and Cp_h is the specific heat of the hot fluid.

ν_h is the kinematic viscosity or momentum diffusivity of the hot fluid and α_h is the thermal diffusivity of the hot fluid and Pr_h is the Prandtl number of the hot fluid:

$$\nu_h = \frac{\mu_h}{\rho_h}, \tag{6}$$

$$\alpha_h = \frac{k_h}{\rho_h Cp_h}, \tag{7}$$

$$Pr_h = \frac{\nu_h}{\alpha_h}. \tag{8}$$

$Rf_c = 0.00018$ and $Rf_h = 0.00053$ are the fouling factors of the cold and hot fluids, respectively. $N_t = 63$ (original value) is the number of plates used in the reference work [1], $\rho_c = 993.8$ kg/m^3 is the specific mass (density) of the cold fluid, $\mu_c = 0.725 \cdot 10^{-3}$ is the dynamic viscosity of the cold fluid, $k_c = 0.610$ is the thermal conductivity of the cold fluid and $Cp_c = 4183$ is the specific heat of the cold fluid.

ν_c is the kinematic viscosity or momentum diffusivity of the cold fluid and α_c is the thermal diffusivity of the cold fluid and Pr_c is the Prandtl number of the cold fluid:

$$\nu_c = \frac{\mu_c}{\rho_c}, \tag{9}$$

$$\alpha_c = \frac{k_c}{\rho_c Cp_c}, \tag{10}$$

$$Pr_c = \frac{\nu_c}{\alpha_c}. \tag{11}$$

$L_V = 1.070$ is the vertical distance between centres of ports, $L_p = 0.858$ is the plate length between ports, $L_w = 0.450$ is the plate width, $L_h = 0.238$ is the horizontal length between centres of ports, $D_P = 0.212$ is the port diameter, $\delta_W = 0.6 \cdot 10^{-3}$ is the plate thickness, $k_W = 17.5$ is the thermal conductivity of the plate, $L_C = 175.56 \cdot 10^{-3}$ is the compressed plate pack length. Pit is the plate pitch:

$$Pit = \frac{L_C}{N_t}, \tag{12}$$

b is the corrugation depth:

$$b = Pit - \delta_W, \tag{13}$$

$\varphi = 1.17$ is the surface enlargement factor, D_h is the hydraulic diameter:

$$D_h = \frac{2b}{\varphi}, \tag{14}$$

A_{ch} is the channel cross-sectional free flow area:

$$A_{ch} = bL_W, \tag{15}$$

N_e is the effective number of heat transfer plates:

$$N_e = N_t - 3, \tag{16}$$

$N_p = 1$ is the number of fluid passes, N_{cp} is the number of channels for one pass:

$$N_{cp} = \frac{N_t - 1}{2N_p}. \tag{17}$$

$A_1 = 0.331$ is the heat transfer area for a plate, A_e is the heat transfer total area:

$$A_e = A_1 N_e, \tag{18}$$

$\boldsymbol{Re_h} = 30.0$ (fixed) is the Reynolds number for hot fluid, G_{ch} is the mass velocity:

$$G_{ch} = \frac{Re_h \mu_h}{D_h}, \tag{19}$$

$\dot{m}_{ch}$ is the mass flow rate per channel:

$$\dot{m}_{ch} = G_{ch} A_{ch}, \tag{20}$$

$\dot{m}_h$ is the total mass flow rate of the hot fluid:

$$\dot{m}_h = \dot{m}_{ch} N_{cp}. \tag{21}$$

$$G_{cc} = \frac{Re_c \mu_c}{D_h}. \tag{22}$$

Re_c is the Reynolds number for cold fluid.

$$\boldsymbol{\dot{m}_{cc} = G_{cc} A_{ch}}, \tag{23}$$

$$\boldsymbol{\dot{m}_c = G_c A_{ch}}, \tag{24}$$

$$C_c = \dot{m}_C p_c, \tag{25}$$

$$C_h = \dot{m}_C p_h, \tag{26}$$

where m_c is the total mass flow rate of the cold fluid and C_h is the thermal capacity of the hot fluid. C_{min} is the minimum thermal capacity between the hot and cold fluids:

$$C^* = \frac{C_{min}}{C_{max}}. \tag{27}$$

Equations (1)–(27) include the physical property determination and mass flowrates needed for the Nusselt calculation. In Table 2, the parameters determined by Skočilas and Palaziuk [1] and for Kumar correlation [3] are presented.

2.1. Equations for no explicit angle in the expressions of Nusselt number

This section presents the Equations (28)–(38) that depend only on the coefficients and exponents shown in Table 2. Nu_c is the Nusselt number for cold fluid:

$$Nu_c = c_2 Re_c^n Pr_c^m \left(\frac{\mu_c}{\mu_W}\right)^x, \tag{28}$$

$$Nu_h = c_2 Re_h^n Pr_h^m \left(\frac{\mu_h}{\mu_W}\right)^x. \tag{29}$$

β	C_2	n	m	x
No angle (Kumar)	0.348	0.663	1/3	0.17
30°	0.14	0.64	0.39	0.1
45°	0.14	0.645	0.395	0.1
60°	0.14	0.65	0.40	0.1

Table 2. Coefficient and exponents for the expression of Nusselt [2] determined by Skočilas and Palaziuk [1].

h_h is the coefficient of heat convection for hot fluid:

$$h_c = \frac{Nu_c k_c}{D_h}, \tag{30}$$

$$h_h = \frac{Nu_h k_h}{D_h}. \tag{31}$$

Uo is the global heat transfer coefficient:

$$Uo = \frac{1}{\frac{1}{h_c} + \frac{1}{h_h} + \frac{\delta_W}{k_W} + Rf_c + Rf_h}. \tag{32}$$

$$\boldsymbol{NTU} = \frac{UoA_e}{c_{min}}, \tag{33}$$

where NTU is the number of thermal units associated with the heat exchanger and A_e is the total heat transfer area, established by Equation (18). ε_T is the thermal effectiveness:

$$\varepsilon_T = \frac{1 - e^{-NTU(1-C^*)}}{1 + C^* e^{-NTU(1-C^*)}}. \tag{34}$$

$\dot{Q}$ is the actual heat transfer rate and Q_{max} is the maximum heat transfer rate:

$$\dot{Q} = \varepsilon_T C_{min}(Th_i - Tc_i), \tag{35}$$

$$\dot{Q}_{max} = C_{min}(Th_i - Tc_i). \tag{36}$$

Tc_o and Th_o are the outlet temperatures for cold and hot fluids, respectively:

$$Tc_o = Tc_i + \frac{\dot{Q}}{\dot{m}_c Cp_c}, \tag{37}$$

$$Th_o = Th_i + \frac{\dot{Q}}{\dot{m}_h Cp_h}, \tag{38}$$

3. Equations for explicit angle in the expressions of Nusselt number

This section introduces several parameters (39)–(55) that explicitly depend on the chevron inclination angle, emphasizing the Nusselt numbers (56) and (57).

β is the chevron inclination angle:

$$\beta = \frac{\pi\beta}{180}, \quad \text{[rad]}, \tag{39}$$

l is the corrugation wavelength:

$$l = Pit \sin\beta, \tag{40}$$

L_{furr} and L_{long} are the furrow and longitudinal flow components:

$$L_{furr} = \frac{l}{\sin 2\beta}, \tag{41}$$

$$L_{long} = \frac{l}{\sin\beta}. \tag{42}$$

XX is the ratio corrugation depth:

$$XX = \frac{b}{Pit}. \tag{43}$$

$D_{h\,sin\,e}$ is the hydraulic dynamic diameter of a sine duct:

$$D_{h\sin e} = (0.149\,XX^3 - 0.623\,XX^2 + 1.087\,XX - 0.0014)l, \tag{44}$$

$A_{ch\sin e}$ is the channel cross-section transverse to the furrow:

$$A_{ch\sin e} = A_{ch}\cos\beta. \tag{45}$$

$$u_{\sin ec} = \frac{\dot{m}_{cc}}{\rho_c A_{ch\sin e}}, \tag{46}$$

$$u_{\sin eh} = \frac{\dot{m}_{ch}}{\rho_h A_{ch\sin e}}, \tag{47}$$

$$Re_{\sin ec} = \frac{2u_{\sin ec}D_{h\sin e}}{\nu_c}, \tag{48}$$

$$Re_{\sin eh} = \frac{2u_{\sin eh}D_{h\sin e}}{\nu_h}. \tag{49}$$

$$C = 2.6624\,XX^4 - 10.586\,XX^3 + 11.262\,XX^2 - 1.036\,XX + 9.6, \tag{50}$$

$$K_{einf} = 5.888\,XX^4 + 9.4611\,XX^3 - 4.248\,XX^2 - 0.1333\,XX + 2.648, \tag{51}$$

$$K_{dinf} = 1.7237\,XX^4 + 2.7669\,XX^3 - 1.2651\,XX^2 - 0.0097\,XX + 1.512, \tag{52}$$

$$K_{\inf} = 2(K_{einf} - K_{dinf}), \tag{53}$$

$$B = \frac{K_{\inf}D_{h\sin e}}{4l_{furr}}. \tag{54}$$

f_{appc} is the apparent friction coefficient:

$$f_{appc} = \frac{C}{Re_{\sin ec}} + B. \tag{55}$$

$$Nu_{c\sin e} = 0.40377\left(4f_{appc}Re^2_{\sin ec} + Pr_c\frac{D_{f\sin e}}{l_{furr}}\right)^{1/3}, \tag{56}$$

$$Nu_{h\sin e} = 0.40377\left(4f_{apph}Re^2_{\sin eh} + Pr_h\frac{D_{f\sin e}}{l_{furr}}\right)^{1/3}. \tag{57}$$

Then, the overall thermal transfer coefficient $U_{o\sin e}$, number of transfer units $NTU_{\sin e}$, thermal effectiveness $\varepsilon_{T\sin e}$, and thermal flux $\dot{Q}_{\sin e}$, can be calculated with Equations (58)–(65)).

$h_{c\sin e}$ is the coefficient of heat convection for cold fluid and $h_{h\sin e}$ is the coefficient of heat convection for hot fluid:

$$h_{c\sin e} = \frac{Nu_{c\sin e}k_c}{D_{h\sin e}}, \tag{58}$$

$$h_{h\sin e} = \frac{Nu_{h\sin e}k_h}{D_{h\sin e}}. \tag{59}$$

Uo is the global heat transfer coefficient and $\varepsilon_{T\sin e}$ is the thermal effectiveness:

$$Uo = \frac{1}{\frac{1}{h_{c\sin e}} + \frac{1}{h_{h\sin e}} + \frac{\delta_W}{k_W} + Rf_c + Rf_h}. \tag{60}$$

$$NTU_{\sin e} = \frac{Uo_{\sin e}A_e}{C_{min}}, \tag{61}$$

$$\varepsilon_{T\sin e} = \frac{1 - e^{-NTU_{\sin e}(1-C^*)}}{1 + C^*e^{-NTU_{\sin e}(1-C^*)}}. \tag{62}$$

$\dot{Q}_{\sin e}$ is the actual heat transfer rate:

$$\dot{Q}_{\sin e} = \varepsilon_{T\sin e}C_{\min}(Th_i - Tc_i). \tag{63}$$

Tc_o and Th_o are the outlet temperatures for cold and hot fluids, respectively:

$$Tc_o = Tc_i + \frac{\dot{Q}_{\sin e}}{\dot{m}_c Cp_c}, \tag{64}$$

$$Th_o = Th_i + \frac{\dot{Q}_{\sin e}}{\dot{m}_h Cp_h}. \tag{65}$$

4. Results and discussion

The results presented in this work are strongly dependent on the experimental parameters determined by Neagu and Koncsag [2]. In addition to the physical and geometric parameters, the most significant influence on obtaining the results are Reynolds number, inlet temperatures, and heat exchanger plates. The Reynolds number range adopted for cold fluid is obtained from Table 5 of reference [2], i.e. $Re_c = 979 < Re < Re_c = 1530$. The Reynolds number for the hot fluid was kept fixed, equal to 30. The original number of plates, taken from Table 1, equals to 63. The inlet temperatures of the hot and cold fluids are equal to 110 °C and 30 °C, respectively. The angle of inclination used in the experiment is equal to 30 °C.

Figure 2 presents the apparent friction factor as a function of the Reynolds number. The angles under analysis are equal to $\beta = 30°$, $\beta = 45°$, and $\beta = 60°$. The highlight is for the angle equal to 30° since the friction factor variation range is compatible with the results of Figure 3 of reference [2]. The results graphically presented in reference [2] show that the

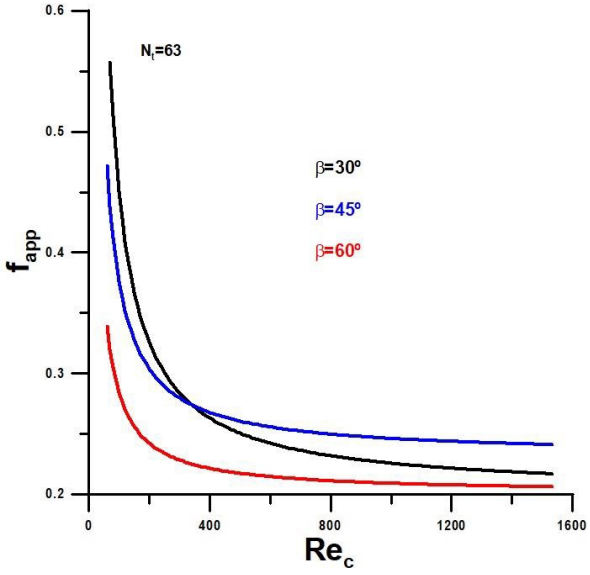

FIGURE 2. Apparent friction coefficient versus Reynolds number with slope angles as parameters.

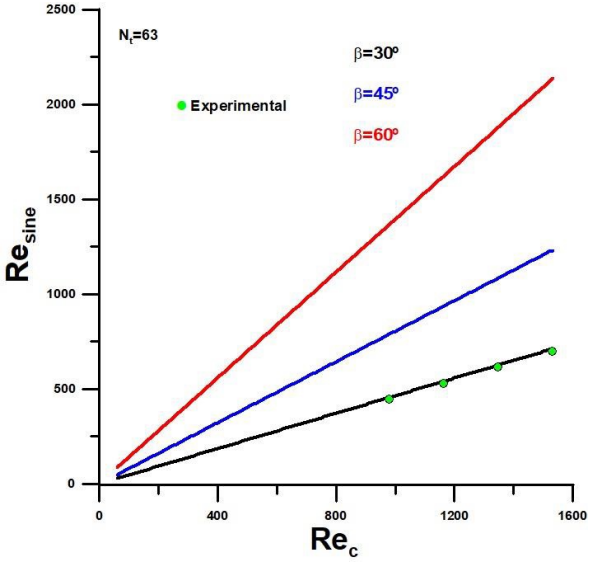

FIGURE 3. Resine versus Reynolds number for cold fluid (Experimental Ref. [2]).

lower limit value for the friction factor is equal to $f_{app} = 0.2$. In this specific situation (chevron angle equal to $\beta = 30°$), the smallest value for the Reynolds number is equal to $Re_c = 60$, and the largest is equal to $Re_c = 1530$. The values obtained for angles equal to $\beta = 45°$ and $\beta = 60°$ show a slight variation concerning the reference angle but are compatible with the values and the trend presented by this one.

The relationship between the Reynolds numbers used in the expressions to determine the Nusselt numbers is shown in Figure 4, for a number of plates equal to $N_T = 63$. The Reynolds $Re_{\sin e}$ number is dependent on the chevron in the inclination angle. The graph shows the relationship for the Reynolds number between $Re_c = 60$ and $Re_c = 1530$. The experimental values are taken from the reference [2], within

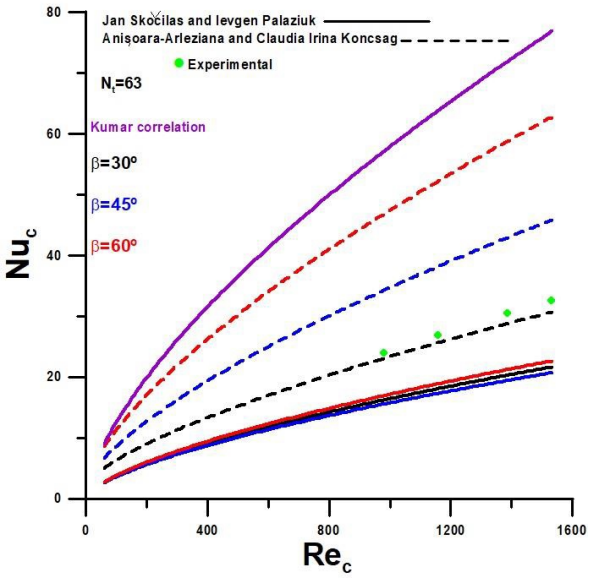

FIGURE 4. Nusselt number versus Reynolds number for cold fluid [1, 2].

the Reynolds number range between $Re_c = 979$ and $Re_c = 1530$, for an inclination angle equal to $\beta = 30°$. The $\beta = 46°$ and $\beta = 60°$ angles are included in the analysis to compare and analyse the theoretical model.

The Nusselt number as a function of the Reynolds number, with slope angles as parameters, is represented in Figure 4. The models under analysis, already described above, were developed by Skočilas and Palaziuk [1], Neagu and Koncsag [2], and Kumar (in [3]). In Figure 4, the experimental values for an angle of $\beta = 30°$ and Reynolds number in the range of $Re_c = 979$ to $Re_c = 1530$ are highlighted. The results obtained through the Skočilas and Palaziuk [1] model do not show great dispersion concerning the angles of inclination and present values significantly lower than the other models. Regarding the model developed by Neagu and Koncsag [2], a significant dispersion can be observed between the values obtained for the angles under analysis. In this case, the values for the Nusselt number increase with the angle of inclination. Regarding the Kumar correlation, regardless of the angle of inclination, it can be observed that the Nusselt number surpasses the other two models under analysis.

Figure 5 shows the global heat transfer coefficient for the models under analysis. It is noteworthy that the global heat transfer coefficient carries information related to the hot fluid and has a value for a Reynolds number equal to $Re_h = 30$. The results obtained through reference [3] do not present great numerical dispersion within the wide range of values obtained by the models. The highlight is the Kumar correlation, with intermediate values between the two models. There is a great difference between the models.

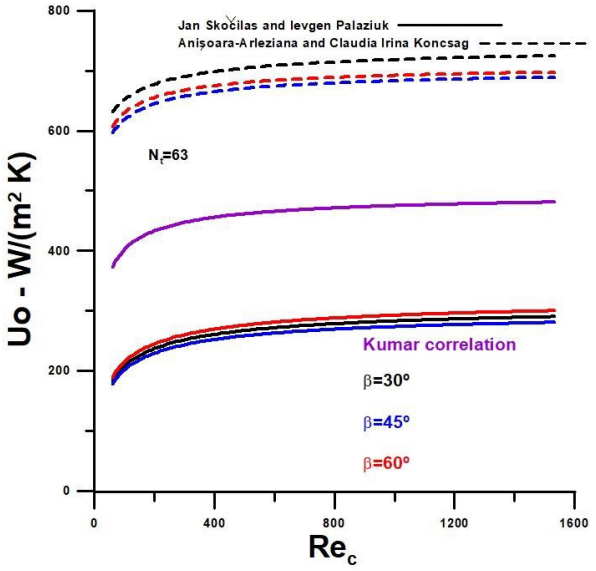

Figure 5. Global heat transfer coefficient versus Reynolds number for cold fluid [2].

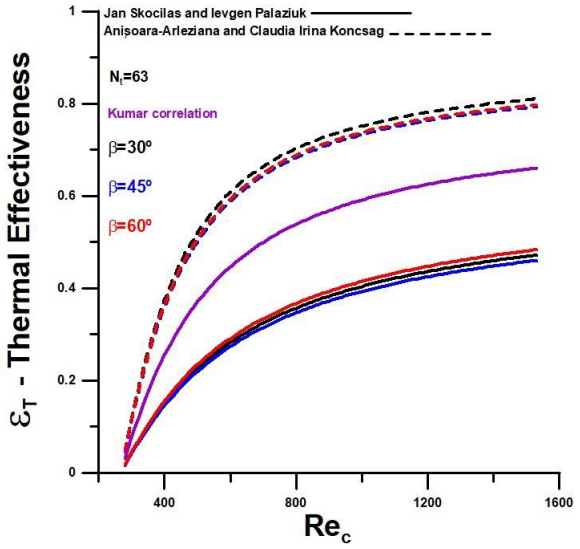

Figure 6. Thermal effectiveness versus Reynolds number for cold fluid [1, 2].

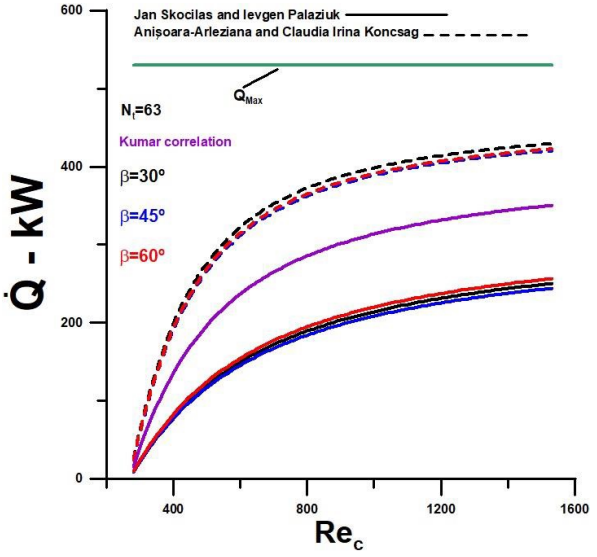

Figure 7. Heat transfer rate versus Reynolds number for cold fluid [2].

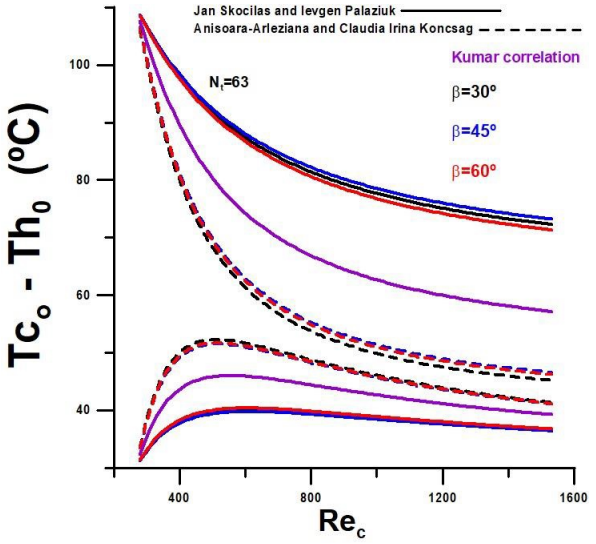

Figure 8. Outlet temperatures versus Reynolds number for cold fluid [2].

As expected, thermal effectiveness, represented by Figure 6, presents a behaviour similar to that obtained for the global heat transfer coefficient. Again, the attention is drawn to the great dispersion between the models, with significantly high values obtained through the reference model [1] concerning the reference values [3]. The effectiveness obtained by Neagu and Koncsag [2] is practically double that of the effectiveness obtained by the model developed by Skočilas and Palaziuk [1]. The Kumar model presents intermediate values, slightly closer to the results obtained through the reference [1].

Figure 7 shows the heat transfer rate and demonstrates, as already observed in Figure 5, that for plates equal to $N_t = 63$ and within the analysed flow rate, the maximum rate theoretically possible is significantly different from the values obtained by the model associated with reference [2], the least conservative of the three under analysis.

Figures 8 and 9 show outlet temperatures for the fluids. The temperatures represented in Figure 8 demonstrate that the model developed and presented through reference [2], with an angle of 30° and plate number equal to $N_t = 63$, is close to the best possible result of the analysed heat exchanger. However, the model developed by Kumar tends to approach these results for higher flow rates. Figure 9 shows the outlet temperature for the hot fluid and demonstrates that the trend presented by the profiles is similar for all of them. The highlight for the model developed by Kumar shows intermediate values to the other two models. The flow variation is more significant as an influence on the thermal performance of the heat exchanger than the angle of inclination.

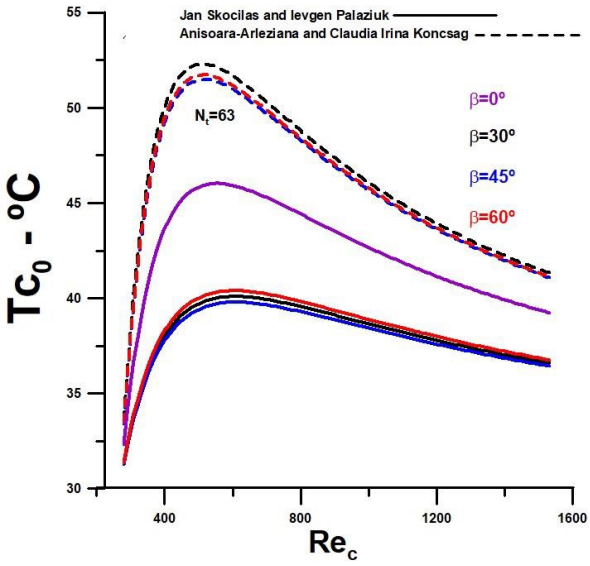

FIGURE 9. Outlet temperature for cold fluid versus Reynolds number for cold fluid.

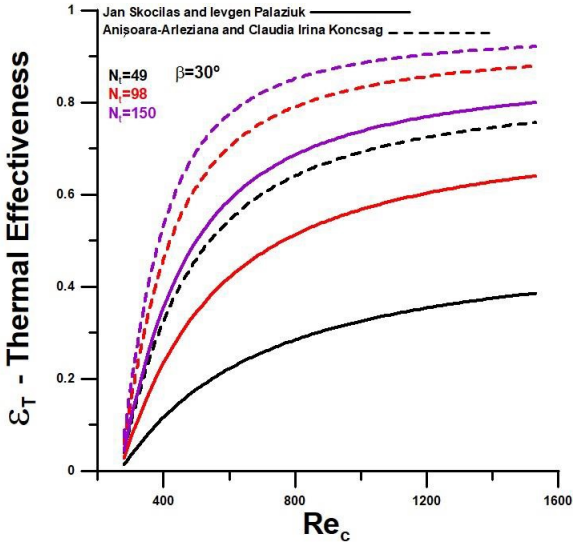

FIGURE 10. Thermal effectiveness versus Reynolds number for cold fluid with number of plates as a parameter.

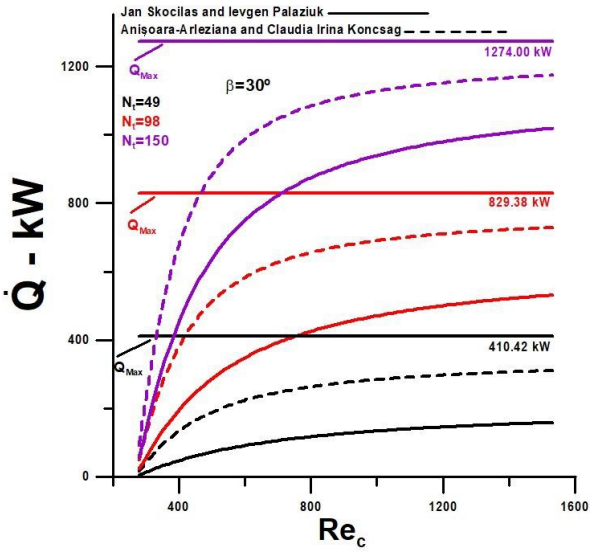

FIGURE 11. Heat transfer rate versus Reynolds number for cold fluid with the number of plates as a parameter [1].

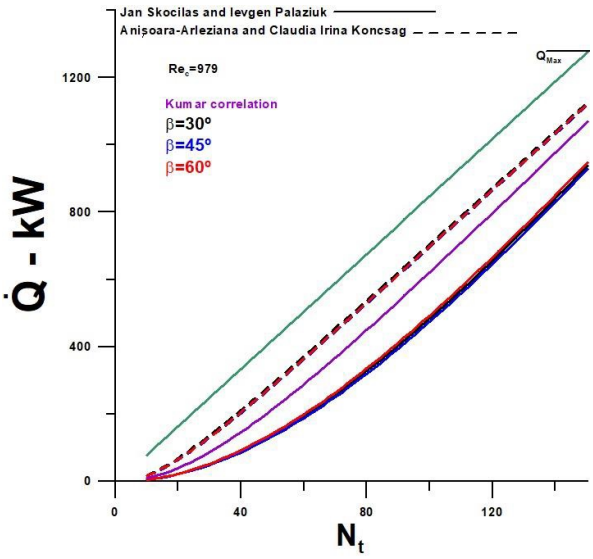

FIGURE 12. Heat transfer rate versus the number of plates for Reynolds number equal to 979 and with inclination angle as a parameter.

Figure 10 shows the effectiveness for number of plates equal to $N_t = 49$, $N_t = 98$, and $N_t = 150$, and an inclination angle equal to $\beta = 30°$. It can be observed that the differences between the models decrease with the increase in the number of plates. For example, with plates, in the case of the model developed by Neagu and Koncsag [2], the effectiveness is very close to 1, i.e., the heat transfer rate is very close to the maximum theoretically possible value.

The results shown in Figure 11 corroborate what was observed for effectiveness. The heat transfer rate increases with the number of plates and approaches the maximum theoretically possible for a plate number equal to $N_t = 150$ and a Reynolds number equal to $Re_c = 1530$. However, the values obtained for heat transfer rate through the model of Skočilas and Palaziuk [1] are relatively different from the maximum possible for any number of plates within the range under analysis.

Figures 12 and 13 show results for heat transfer rate as a function of the number of plates, for Reynolds numbers equal to $Re_c = 979$ and $Re_c = 1530$, with slope angles as parameters. The heat transfer rate increases with the number of plates and approaches the maximum for the highest flow rates under analysis. For high plate numbers, the model developed by Kumar is close to the model presented by Neagu and Koncsag [2]. The inclination angle does not significantly affect the heat transfer rate, regardless of the model analysed.

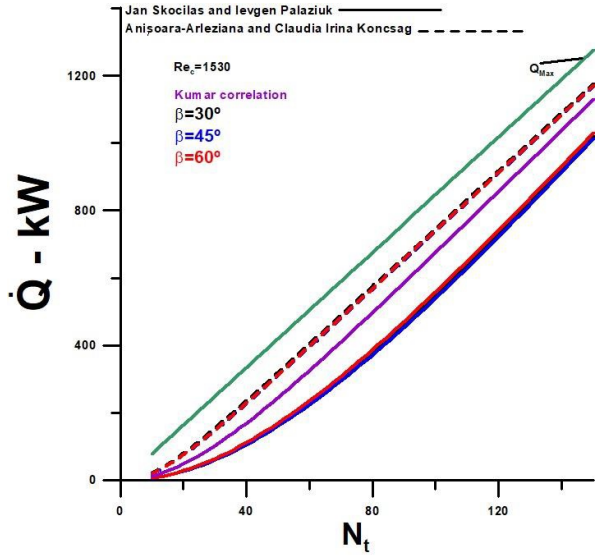

Figure 13. Heat transfer rate versus the number of plates for Reynolds number equal to 1530 and with inclination angle as a parameter.

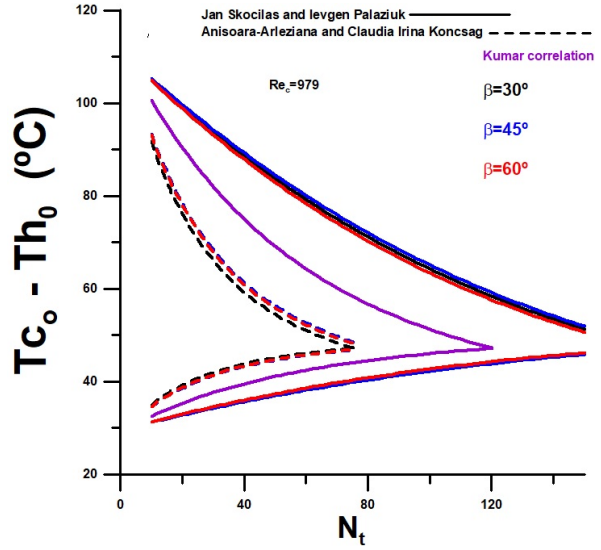

Figure 14. Outlet temperatures of fluids versus the number of plates for Reynolds number equal to 979 and with inclination angle as a parameter [1, 2].

The graphical results presented in Figures 14 and 15 show the outlet temperatures for the cold and hot fluids as a function of Reynolds numbers equal to $Re_c = 979$ and $Re_c = 1530$, respectively, with slope angles as parameters. The number of plate limit depends on the model used in the analysis since the second law of thermodynamics imposes a physical limitation. It is observed that this limit depends on the flow rates of the fluids and, again, is not much influenced by the chevron tilt angle. As the model presented by Neagu and Koncsag [2] significantly approaches 100 % of effectiveness (ε_1) for both Reynolds numbers under analysis, the maximum possible number of plates is the smallest among the models. In this specific case, the maximum number of plates for

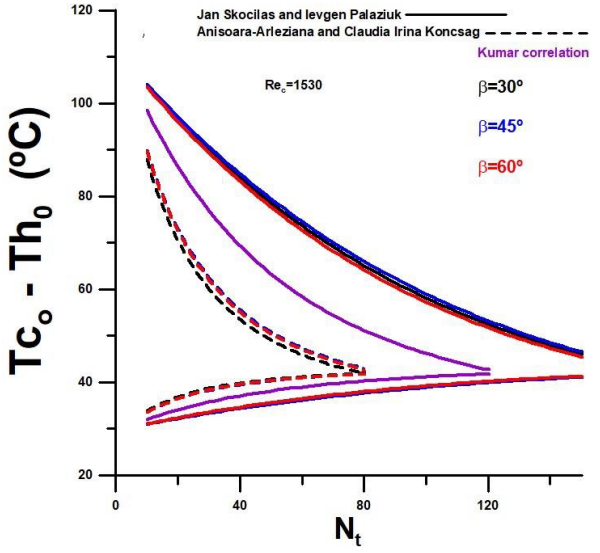

Figure 15. Outlet temperatures of fluids versus the number of plates for Reynolds number equal to 1530 and with inclination angle as a parameter [1, 2].

Reynolds number equal to $Re_c = 979$ is $N_t = 78$, and for Reynolds number equal to $Re_c = 1530$, $N_t = 82$. When it comes to the Kumar model, you can see that the limiting numbers are equal to $N_t = 120$ and $N_t = 122$. As the effectiveness is very low in the case of the model developed by Skočilas and Palaziuk [1], the maximum numbers for both flows under analysis are above $N_t = 150$.

5. Conclusion

The work analysed the influence of the chevron plate inclination angle on the thermal performance of a Gasket plate heat exchanger. Three models were used to determine the Nusselt number through theoretical and experimental correlations. The models were developed by Kumar, Skočilas and Palaziuk [1], and Neagu and Koncsag [2].

Regarding the analysed models, there is a great difference between them. It can be said that the values obtained by the authors are very different from each other. And in this sense, it is concluded that the maximum flow rate and the limit number of plates to be used in the heat exchanger strongly depend on the used model.

Based on the results presented, the model developed by Neagu and Koncsag [2] is the most efficient and effective. It obtains final results for exit temperatures very close to the other models, developed by Kumar and Skočilas and Palaziuk [1], with a smaller number of plates and a lower flow rate for the cold fluid. The model developed by Kumar does not explicitly consider the inclination angle, and the results obtained are intermediate to the other two and slightly approach the model developed by Neagu and Koncsag [2] for high flow rates.

The flow rate variation is more significant as an influence on the thermal performance of the heat ex-

changer than the angle of inclination, and the number of plates to be used in the heat exchanger are the other main factors responsible for the thermal performance.

The number of plates used in reference [2], $N_t = 63$, is quite adequate, following the analyses performed.

Based on the results obtained, the need for new theoretical and experimental works related to the influence of chevron inclination angles is evident.

List of symbols

A_{ch} channel cross-sectional free flow area [m^2]
A_e heat transfer total area [m^2]
$A_{ch\,\sin e}$ channel cross-section transverse to the furrow [m^2]
b corrugation depth [m]
Cp_c specific heat of the cold fluid [J/(kg K)]
Cp_h specific heat of the hot fluid [J/(kg K)]
C_h thermal capacity of the hot fluid [W/K]
C_{min} minimum thermal capacity between the hot and cold fluids [W/K]
$C^* = C_{min}/C_{max}$
D_h hydraulic diameter [m]
$D_{h\,\sin e}$ hydraulic dynamic diameter of a sine duct [m]
D_P port diameter [m]
f_{app} apparent friction coefficient
G_{ch} mass velocity of the hot fluid [kg/(m^2 s)]
G_{cc} mass velocity of the cold fluid [kg/(m^2 s)]
h_h coefficient of heat convection for hot fluid [W/(m^2 K)]
h_c coefficient of heat convection for cold fluid [W/(m^2 K)]
$h_{c\,\sin e}$ coefficient of heat convection for cold fluid [W/(m^2 K)]
$h_{h\,\sin e}$ coefficient of heat convection for hot fluid [W/(m^2 K)]
k_h thermal conductivity of the hot fluid [W/(m K)]
k_c thermal conductivity of the cold fluid [W/(m K)]
k_W thermal conductivity of the plate [W/(m K)]
l the corrugation wavelength
L_C compressed plate pack length [m]
L_h horizontal length between centres of ports [m]
L_p plate length between ports [m]
L_V vertical distance between centres of ports [m]
L_w plate width [m]
L_{furr} furrow flow components [m]
L_{long} longitudinal flow components [m]
$\dot{m}_{ch}$ mass flow rate per channel [kg/s]
$\dot{m}_c$ total mass flow rate of the cold fluid [kg/s]
$\dot{m}_h$ total mass flow rate of the hot fluid [kg/s]
N_{cp} number of channels for one pass
N_e effective heat transfer number of plates
N_p number of fluid passes
N_t number of plates
Nu_c Nusselt number for cold fluid
Nu_h Nusselt number for hot fluid
$Nu_{c\,\sin e}$ Nusselt number for cold fluid for a sine duct
$Nu_{h\,\sin e}$ Nusselt number for hot fluid for a sine duct
Pr_c is the Prandtl number of the cold fluid
Pr_h is the Prandtl number of the hot fluid
Pit plate pitch [m]
$\dot{Q}$ actual heat transfer rate [W]
$\dot{Q}_{max}$ maximum heat transfer rate [W]
$\dot{Q}_{\sin e}$ actual heat transfer rate [W]
Re_c Reynolds number for cold fluid
Re_h Reynolds number for hot fluid
$Re_{\sin ec}$ Reynolds number for cold fluid in a sine duct
$Re_{\sin eh}$ Reynolds number for hot fluid in a sine duct
Tci inlet temperature of water [°C]
Thi inlet temperature of vegetable oil [°C]
Tc_o outlet temperature for cold fluid [°C]
Th_o outlet temperature for hot fluid [°C]
Uo global heat transfer coefficient [W/(m^2 K)]
$Uo_{\sin e}$ global heat transfer coefficient of a duct sine [W/(m^2 K)]

Greek symbols

α_c thermal diffusivity of the cold fluid [m^2/s]
β corrugation angle of the plate
φ area enlargement factor
ρ density of the fluid [kg/m^3]
μ dynamic viscosity of fluid [kg/(m s)]
ν_c the kinematic viscosity of the cold fluid [m^2/s]
ε effectiveness

Acronyms

CFD computational fluid dynamics
GPHE gasket plate heat exchanger
NTU number of thermal units

References

[1] J. Skočilas, I. Palaziuk. CFD simulation of the heat transfer process in a chevron plate heat exchanger using the SST turbulence model. *Acta Polytechnica* **55**(4):267–274, 2015. https://doi.org/10.14311/AP.2015.55.0267.

[2] A.-A. Neagu, C. I. Koncsag. Model validation for the heat transfer in gasket plate heat exchangers working with vegetable oils. *Processes* **10**(1):102, 2022. https://doi.org/10.3390/pr10010102.

[3] S. Kakaç, H. Liu, A. Pramuanjaroenkij. *Heat Exchangers – Selection, Rating, and Thermal Design.* CRC Press, Taylor & Francis Groupe, Boca Raton, London, New York, 3rd edn., 2012.

[4] E. Nogueira. Entropy generation analysis in a gasket plate heat exchanger using non-spherical shape of alumina boehmite nanoparticles. *Ovidius University Annals of Chemistry* **33**(1):41–49, 2022. https://doi.org/10.2478/auoc-2022-0006.

[5] L. Tovazhnyanskyy, J. J. Klemeš, P. Kapustenko, et al. Optimal design of welded plate heat exchanger for ammonia synthesis column: An experimental study with mathematical optimisation. *Energies* **13**(11):2847, 2020. https://doi.org/10.3390/en13112847.

[6] D. H. Nguyen, K. M. Kim, T. T. Nguyen Vo, et al. Improvement of thermal-hydraulic performance of plate heat exchanger by electroless nickel, copper and silver

plating. *Case Studies in Thermal Engineering* **23**:100797, 2021. https://doi.org/10.1016/j.csite.2020.100797.

[7] B. Kumar, S. N. Singh. Hydraulic and thermal studies on a chevron type plate heat exchanger. *Thermal Science* **22**(6):2759–2770, 2018. https://doi.org/10.2298/TSCI160324312K.

[8] G. Roxana, P. Sorin, H. Aneta, H. Gheorghe. Study regarding numerical simulation of counter flow plate heat exchanger. In J. Awrejcewicz (ed.), *Numerical Analysis*. IntechOpen, Rijeka, 2011. ISBN 978-953-307-389-7, https://doi.org/10.5772/24113.

[9] M. A. Jamil, T. S. Goraya, H. Yaqoob, et al. Exergoeconomic and normalized sensitivity analysis of plate heat exchangers: A theoretical framework with application. In L. C. Gómez, V. M. V. Flores, M. N. Procopio (eds.), *Heat Exchangers*, chap. 1. IntechOpen, Rijeka, 2021. https://doi.org/10.5772/intechopen.99736.

[10] D. dos S. Ferreira, M. Mantelli, F. Milanese. Wilson plot method to obtain nusselt number for a plate heat exchanger. *Engenharia Térmica (Thermal Engineering)* **19**(2):25–30, 2020. https://doi.org/10.5380/reterm.v19i2.78610.

[11] F. A. Mota, E. Carvalho, M. A. Ravagnani. Modeling and design of plate heat exchanger. In S. N. Kazi (ed.), *Heat Transfer*, chap. 7. IntechOpen, Rijeka, 2015. https://doi.org/10.5772/60885.

[12] G. Anusha, P. S. Kishore. Heat transfer analysis of gasketed plate heat exchanger. *International Journal of Engineering Research* **5**(12):943–947, 2016. https://doi.org/10.17950/ijer/v5s12/1215.

[13] K. Harshal, S. P. Dilpak, V. M. Kundalik. Design optimization algorithm for plate heat exchanger. *International Journal of Current Engineering and Technology* (Special Issue 4):149–155, 2016. https://doi.org/10.14741/Ijcet/22774106/spl.4.2016.31.